


# Enzymatic liquefaction of agarose above the sol–gel transition temperature using a thermostable endo-type $\beta$ -agarase, Aga16B

Jung Hyun Kim<sup>1</sup> · Eun Ju Yun<sup>1</sup> · Nari Seo<sup>2</sup> · Sora Yu<sup>1</sup> · Dong Hyun Kim<sup>1</sup> ·  
Kyung Mun Cho<sup>1</sup> · Hyun Joo An<sup>2</sup> · Jae-Han Kim<sup>3</sup> · In-Geol Choi<sup>1</sup> · Kyoung Heon Kim<sup>1</sup> 

Received: 5 May 2016 / Revised: 14 August 2016 / Accepted: 21 August 2016 / Published online: 24 September 2016  
© Springer-Verlag Berlin Heidelberg 2016

**Abstract** The main carbohydrate of red macroalgae is agarose, a heterogeneous polysaccharide composed of D-galactose and 3,6-anhydro-L-galactose. When saccharifying agarose by enzymes, the unique physical properties of agarose, namely the sol–gel transition and the near-insolubility of agarose in water, limit the accessibility of agarose to the enzymes. Due to the lower accessibility of agarose to enzymes in the gel state than to the sol state, it is important to prevent the sol–gel transition by performing the enzymatic liquefaction of agarose at a temperature higher than the sol–gel transition temperature of agarose. In this study, a thermostable endo-type  $\beta$ -agarase, Aga16B, originating from *Saccharophagus degradans* 2-40<sup>T</sup>, was characterized and introduced in the liquefaction process. Aga16B was thermostable up to 50 °C and depolymerized agarose mainly into neoagarooligosaccharides with degrees of polymerization 4 and 6. Aga16B was applied to enzymatic liquefaction of agarose at 45 °C, which was above the sol–gel transition temperature of 1 % (w/v) agarose (~35 °C) when cooling agarose. This is the first systematic demonstration of

enzymatic liquefaction of agarose, enabled by determining the sol–gel temperature of agarose under specific conditions and by characterizing the thermostability of an endo-type  $\beta$ -agarase.

**Keywords** Red macroalgae · Agarose · Enzymatic liquefaction · Saccharification · Agarase

## Introduction

Marine red macroalgae have been considered as sustainable resource for producing fuels and chemicals due to higher carbohydrates and low or lack of lignin (Wei et al. 2013; Yun et al. 2015, 2016). The main component of red macroalgae is agar that has a hybrid structure with the carbohydrate backbone of galactan consisting of alternating  $\beta$ -D-galactopyranose and  $\alpha$ -L-galactopyranose (Chi et al. 2012; Knutsen et al. 1994). Agarose is the neutral linear polymer as the main fraction of agar. In agarose,  $\beta$ -D-galactose and  $\alpha$ -3,6-anhydro-L-galactose (AHG) alternatively appear and are linked by  $\beta$ -1,4- and  $\alpha$ -1,3-glycosidic bonds (Chi et al. 2012; Knutsen et al. 1994). The average length of agarose is approximately 800 hexose units (Armisen 1991). The monomeric sugar units of agar backbones are often derivatized by substitution with sulfate ester, methyl, or pyruvate acetal groups (Lahaye et al. 1989). Since agarose is the major source of carbohydrates in red macroalgae, efficient saccharification of agarose is important for its industrial use (Yun et al. 2016). To saccharify agarose, either chemical or enzymatic hydrolysis can be used.

To enzymatically saccharify agarose, the unique characteristics of agarose need to be taken into account: (i) sol–gel transition and (ii) the near-insolubility in water below boiling temperature. Agarose in water can exist as a solid in either sol or gel form. When heated agarose in water is cooled down, its

Jung Hyun Kim and Eun Ju Yun contributed equally to this work.

**Electronic supplementary material** The online version of this article (doi:10.1007/s00253-016-7831-y) contains supplementary material, which is available to authorized users.

✉ Kyoung Heon Kim  
khekim@korea.ac.kr

- <sup>1</sup> Department of Biotechnology, Graduate School, Korea University, Seoul 02841, South Korea
- <sup>2</sup> Graduate School of Analytical Science and Technology and Asia-Pacific Glycomics Reference Site, Chungnam National University, Daejeon 34134, South Korea
- <sup>3</sup> Department of Food and Nutrition, Chungnam National University, Daejeon 34134, South Korea

sol state is transformed into a gel state, which is called a sol–gel transition (Fujii et al. 2000). Although agarose in sol and gel are both solid, the physical shapes of sol and gel are completely different (Fig. 1). A sol of agarose with water is composed of solid particles dispersed in the continuous water phase, but a gel of agarose with water composed of a continuous polymeric network in which water is confined in each cavity (Brinker and Scherer 2013). Possibly due to the smaller specific surface area and the restricted fluid movement in the gel form of agarose, the sol form of agarose has higher accessibility to enzymes than the gel form of agarose. Therefore, to facilitate the enzymatic saccharification of agarose, it is advantageous to keep agarose in the sol state above the sol–gel temperature of agarose, in which the sol–gel temperature varies depending on the concentration of agarose in water (Nussinovitch 1997).

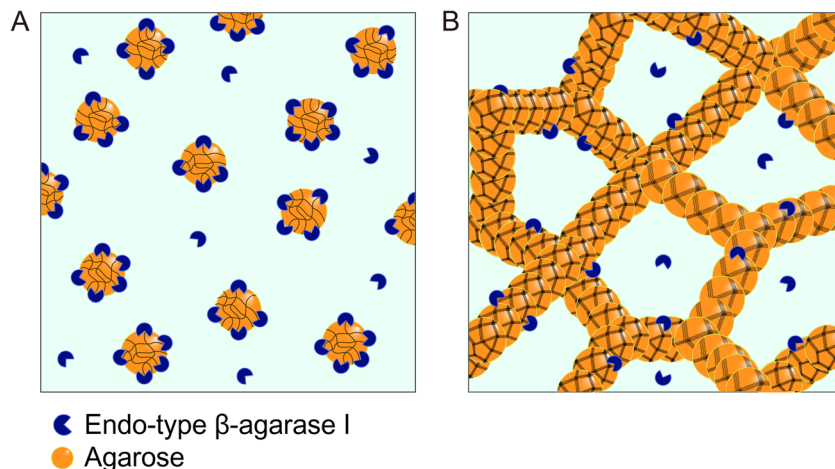
The second problem with the enzymatic saccharification of agarose is posed by the near-insolubility of agarose in water, as agarose is soluble only in hot water near its boiling temperature (Armisen and Galatas 1987; Nussinovitch 1997). To increase the solubility of agarose in water, chemical prehydrolysis of agarose is performed to transform agarose into agarooligosaccharides (AOSs), which are more soluble in water than agarose (Kim et al. 2012, 2013). When using acid catalysts,  $\alpha$ -1,3-glycosidic linkages of agarose are preferentially cleaved and even-numbered AOSs with D-galactose at the nonreducing ends are predominantly produced (Kim et al. 2013; Lee et al. 2014). These AOSs are then hydrolyzed to the monomeric sugars via multiple enzymatic saccharification steps using an exo-type  $\beta$ -agarase (Kim et al. 2010), a neoagarobiose hydrolase (NABH; Kim et al. 2012; Yun et al. 2013), and the agarolytic  $\beta$ -galactosidase (ABG) (Lee et al. 2014). The drawbacks of this combined process of acid prehydrolysis and enzymatic saccharification are as follows: (i) the formation of salts, such as gypsum, as a result of the neutralization of acid prehydrolysate (Kim

et al. 2012); (ii) the formation of 5-hydroxymethylfurfural (5-HMF) from the degradation of heat-labile AHG during acid prehydrolysis at high temperatures (Lee et al. 2015); and (iii) the additional use of ABG, which is required to hydrolyze the agarotriose that results from the acid prehydrolysis and enzymatic saccharification by the exo-type  $\beta$ -agarase (Lee et al. 2015).

To overcome the obstacles described above, it is necessary to replace acid prehydrolysis with enzymatic liquefaction. In the  $\beta$ -agarase system, agarose is converted to neoagarooligosaccharides (NAOSs) by the endo-type  $\beta$ -agarase belonging to glycoside hydrolase 16 (GH16) and 86 (GH86) families (Ekborg et al. 2006). The NAOSs are then hydrolyzed to neoagarobiose (NAB) by the exo-type  $\beta$ -agarase (Kim et al. 2010), and the monomeric sugars (i.e., AHG and D-galactose) are produced by NABH (Ha et al. 2011). Exo-type  $\beta$ -agarase and NABH belong to GH50 and GH117, respectively. To replace the chemical prehydrolysis with enzymatic liquefaction using endo-type  $\beta$ -agarase, the first hydrolysis reaction by the endo-type  $\beta$ -agarase needs to be performed at a temperature higher than that of the sol–gel transition of agarose in water; this is because the accessibility of agarose to enzymes is much higher in sol than in gel. Unfortunately, most kinds of endo-type  $\beta$ -agarase have been reported to lose enzymatic activities over 55 °C (Chi et al. 2014a; Li et al. 2015; Park et al. 2015; Temuujin et al. 2011). Therefore, thermostability of endo-type  $\beta$ -agarase is highly desirable for the effective enzymatic liquefaction of agarose.

Here, a thermostable endo-type  $\beta$ -agarase belonging to GH16, Aga16B, originating from *Saccharophagus degradans* 2-40<sup>T</sup> (Kim et al. 2012; Ko et al. 2012), was characterized and evaluated for application to the enzymatic liquefaction of agarose. More specifically, the thermostability of Aga16B was tested, in a temperature range higher than the sol–gel transition temperature of agarose, to determine whether Aga16B can be used at a temperature at which agarose exists in the

**Fig. 1** Schematic diagram of the simplified **a** sol and **b** gel states of agarose particles in aqueous solution of enzyme



sol state. Thus, this study tests the feasibility of using a  $\beta$ -agarase as an alternative to acid prehydrolysis for enzymatic liquefaction of agarose.

## Materials and methods

### Cloning of *aga16B* originating from *S. degradans* 2-40<sup>T</sup> and multiple amino acid sequence alignment

*S. degradans* 2-40<sup>T</sup> (ATCC 43961) was grown in a defined minimal medium containing 2.3 % (w/v) synthetic sea salts (Aquarium Systems, Mentor, OH, USA), 0.2 % (w/v) glucose, 0.1 % (w/v) yeast extract, and 0.05 % (w/v) ammonium chloride in a 50 mM Tris-HCl buffer (pH 7.4) at 30 °C and 200 rpm for 12 h. The genomic DNA of *S. degradans* 2-40<sup>T</sup> was extracted using a commercial DNA isolation kit (Bioneer, Daejeon, Korea), and the gene *aga16B* (Sde\_1175 [UniProt accession no. Q21LJ2]), was amplified by PCR using the following primers: *aga16B*-N, 5'-AAAGGATCCATGGCAGATTGGGACGGAATT-3', and *aga16B*-C, 5'-AAAGCGGCCGCGTTGCTAAGCGTGAAGCTTATCTA-3'. The predicted signal sequence at the N-terminus of *aga16B* (1–19 amino acids) was removed to facilitate protein expression in host cells. The restriction sites of *Bam*HI and *Not*I were added at the 5' and 3' regions of the N- and C-terminal ends, respectively. The PCR product and pET21a (Novagen, Madison, WI, USA) were digested with *Bam*HI and *Not*I and ligated together using a T4 DNA ligase (BioLabs, Ipswich, MA, USA). The resulting pET21a vectors harboring *aga16B* gene were transformed into *Escherichia coli* BL21(DE3) (Novagen, Madison, WI, USA). Multiple amino acid sequence alignment of Aga16B with the known  $\beta$ -agarases belonging to GH16 from different species was performed by Clustal Omega program (Sievers et al. 2011).

### Overexpression and purification of the recombinant Aga16B

To produce the recombinant protein Aga16B, *E. coli* BL21(DE3) harboring the *aga16B* gene were grown at 37 °C in Luria-Bertani broth (Merck KGaA, Darmstadt, Germany) containing 100  $\mu$ g/ml of ampicillin until the midexponential phase of growth. Then, protein expression was induced by adding 0.5 mM isopropyl- $\beta$ -D-thiogalactopyranoside (Sigma-Aldrich, St. Louis, MO, USA) at 16 °C for 16 h. The cells were harvested by centrifugation at 8000 $\times$ g for 20 min at 4 °C, and the cell pellet was resuspended into a 20 mM Tris-HCl buffer (pH 7.4). The resuspended cells were disrupted using a sonicator (Branson, Gunpo, Korea), and the supernatant was collected by centrifugation at 16,000 $\times$ g for 1 h at 4 °C. The recombinant Aga16B was purified by using a His-Trap column (GE Healthcare, Buckinghamshire, UK), and the identity of the

purified Aga16B was verified by SDS-PAGE using its theoretical molar mass of 63.7 kDa (Fig. 2). The purified Aga16B was concentrated using an Amicon ultrafiltration membrane (molecular weight cutoff of 30 kDa; Millipore, Billerica, MA, USA), and the protein concentration was measured using a bicinchoninic acid (BCA) protein assay kit (Thermo Fisher Scientific, San Jose, CA, USA).

### Assay of enzymatic activity of Aga16B

The agarase activity of Aga16B was measured under the following reaction conditions. A certain amount of Aga16B was incubated in 3 ml of a 20 mM Tris-HCl buffer (pH 7.0) containing 1 % (w/v) agarose at 45 °C for 30 min. After the enzymatic reaction was terminated by incubating the postreaction mixture at 95 °C for 1 min, the amount of the reducing sugars in the reaction mixture was measured by a dinitrosalicylic acid (DNS) reagent at 540 nm (Miller 1959), using D-galactose as a standard. One unit (U) of Aga16B activity was defined as the amount of enzyme required to release 1  $\mu$ mol of reducing sugar per minute at the above enzymatic reaction conditions.

### Enzyme characterization and kinetic parameters for Aga16B

To determine the optimal temperature of Aga16B, Aga16B was incubated with 1 % (w/v) agarose in 20 mM Tris-HCl (pH 7.0) for 30 min at various temperatures ranging from 30 to 70 °C. The optimal pH of Aga16B was determined by incubating Aga16B with 1 % (w/v) agarose in buffers with different pHs, such as a 20 mM sodium phosphate buffer (pH 5–7), a 20 mM Tris-HCl buffer (pH 7.5–9), and a 20 mM borate buffer (pH 9.5–11) at 45 °C for 30 min. After

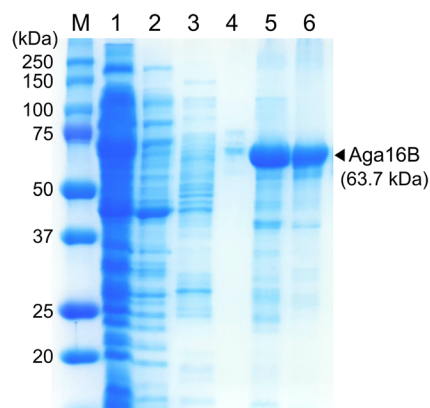


**Fig. 2** SDS-PAGE analysis of purified recombinant Aga16B. Lines: M, protein markers; 1, crude extract; 2, flow-through fraction from crude extract loaded into a His-Trap column; 3, wash fraction from washing the His-Trap column using equilibrium buffer; 4–6, elution fractions from the His-Trap column

the enzymatic reactions, the relative enzymatic activity was measured by determining the amount of reducing sugar using the DNS reagent at 540 nm using galactose as the standard. To measure the thermostability of Aga16B, Aga16B was preincubated at various temperatures ranging from 40 to 65 °C for 0 to 2 h, prior to the enzymatic reaction with agarose. The reaction conditions for measuring the enzyme activities of Aga16B on agarose after the preincubation were the same as described above. To measure the kinetic parameters of Aga16B, the enzymatic reactions were performed with different concentrations of agarose, ranging from 0.5 to 2 % (w/v) in the total reaction mixture volume of 3 ml containing 0.04 mg/ml of purified Aga16B at 45 °C. The reaction times were 6 min for 0.5 and 1 % (w/v) agarose and 10 min for 1.5 and 2 % (w/v) agarose. The values of  $V_{max}$  and  $K_m$  were calculated from the Lineweaver-Burk plot.

#### Analysis of enzymatic reaction products by thin-layer chromatography and high-performance liquid chromatography

To analyze the reaction products of Aga16B on agarose by thin-layer chromatography (TLC), a 1  $\mu$ l aliquot from each reaction mixture was loaded onto silica gel 60 TLC plates (Merck, Darmstadt, Germany), and the plates were developed with *n*-butanol-ethanol-water (3:1:1, v/v/v). The plates loaded with the sample were visualized with 10 % (v/v) H<sub>2</sub>SO<sub>4</sub> and 0.2 % (w/v) naphthoresorcinol in ethanol (Yun et al. 2013). The reaction products of Aga16B on agarose were also analyzed by high-performance liquid chromatography (HPLC; Agilent Technologies, Santa Clara, CA, USA) equipped with a gel permeation column (KS-802; Shodex, New York, NY, USA). HPLC analysis was performed at 80 °C using distilled water as the mobile phase at a flow rate of 0.5 ml/min.

#### Analysis of the enzymatic reaction products by matrix-assisted laser desorption ionization–tandem time-of-flight mass spectrometry

The enzymatic reaction products of Aga16B incubated with agarose were analyzed by matrix-assisted laser desorption ionization–tandem time-of-flight mass spectrometry (MALDI–TOF/TOF MS) using an ultrafleXtreme MALDI–TOF/TOF MS system (Bruker Daltonics, Bremen, Germany). Prior to the analysis, the reaction products of Aga16B were purified by solid-phase extraction using a porous graphitized carbon cartridge (Thermo Fisher Scientific, San Jose, CA, USA) to remove salts and buffer. The purified reaction products of Aga16B were resolubilized in water, and 1.0  $\mu$ l was spotted on a stainless steel target plate, followed by 0.3  $\mu$ l of 0.01 M NaCl and 0.5  $\mu$ l of 0.1 mg/ml 2,5-dihydroxy-benzoic acid (Sigma-Aldrich, St. Louis, MO) in 50 % acetonitrile. The spot was dried under vacuum for more homogeneous

crystallization. MALDI–TOF mass spectra were acquired in a positive mode over the *m/z* range from 500 to 3000 for a total of 2400 laser shots.

To obtain MS/MS data, precursor ions were accelerated to 7.5 kV and selected in a timed ion selector for the fragment ion analysis in the TOF/TOF mode. Fragment ions generated by 1-keV collision energy via collision-induced dissociation (CID) of precursor ions were further accelerated by 19 kV in the LIFT cell, and their masses were analyzed after having them pass through the ion reflector. Argon was used as a collision gas at pressures of  $5.9 \times 10^{-6}$  mbar. Raw MS data and MS/MS data were processed using the flexAnalysis software (version 3.3, Bruker Daltonics, Bremen, Germany).

#### Monitoring sol–gel transition and enzymatic liquefaction of agarose by Aga16B

Sol–gel transition of agarose was monitored by measuring the specific optical rotation of an agarose solution using a polarimeter (JASCO, Easton, PA, USA). To determine the sol–gel transition temperature of agarose, 1 % (w/v) agarose in 20 mM Tris–HCl (pH 7.0) was cooled from 80 to 5 °C. To physically verify the enzymatic liquefaction phase of agarose by Aga16B, the turbidities of 1 % (w/v) agarose before the enzymatic reaction, the reaction mixture, and 20 mM Tris–HCl buffer (pH 7.0) were compared by measuring their absorbances at 600 nm.

## Results

#### Sol–gel transition temperature of agarose

The sol–gel transition of agarose by cooling was monitored by cooling the agarose (1 %, w/v) by measuring the specific optical rotation using the polarimeter (Fig. 3). The agarose was

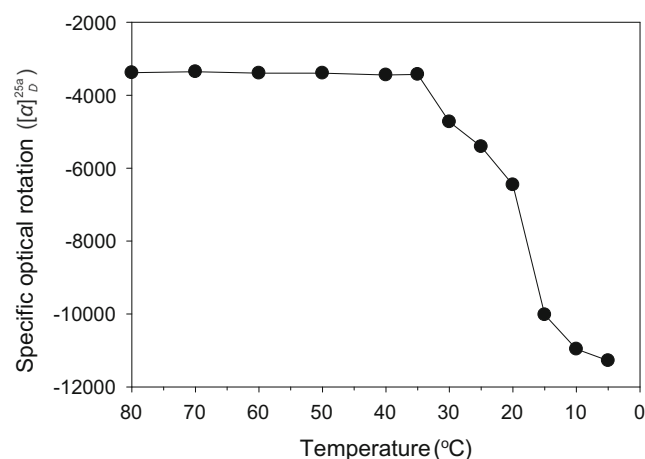


**Fig. 3** Sol–gel transition of agarose by cooling. Sol–gel transition of 1 % (w/v) agarose was monitored by measuring the specific optical rotations

melted at 80 °C, and the sol state of agarose was maintained until it cooled to 35 °C. The sol–gel transition of agarose started occurring at ~35 °C when cooling agarose at a concentration of 1 % (w/v) (Fig. 3). In other words, at a temperature below 35 °C, agarose solidified to gel and the gel structure of agarose became more rigid by being cooled to 5 °C (Fig. 3) (Medina-Esquivel et al. 2008). To perform the enzymatic liquefaction process for 1 % (w/v) agarose more effectively, it is desired to perform the hydrolysis reaction by the endo-type  $\beta$ -agarase over 35 °C, at which agarose is in the sol state. Therefore, it is necessary for the enzyme to be stable over 35 °C without losing its activity.

### Optimal reaction pH and temperature of Aga16B

To determine the optimal reaction pH and temperature of Aga16B for the hydrolysis of agarose, 1 % (w/v) agarose was incubated with Aga16B at different temperatures (30 to 70 °C) and different pHs (pH 5 to 11). Aga16B exhibited high enzymatic activity from 40 to 60 °C (Fig. 4a). Although the enzymatic activity of Aga16B decreased significantly at 65 °C, 54 % of its maximal activity was still maintained

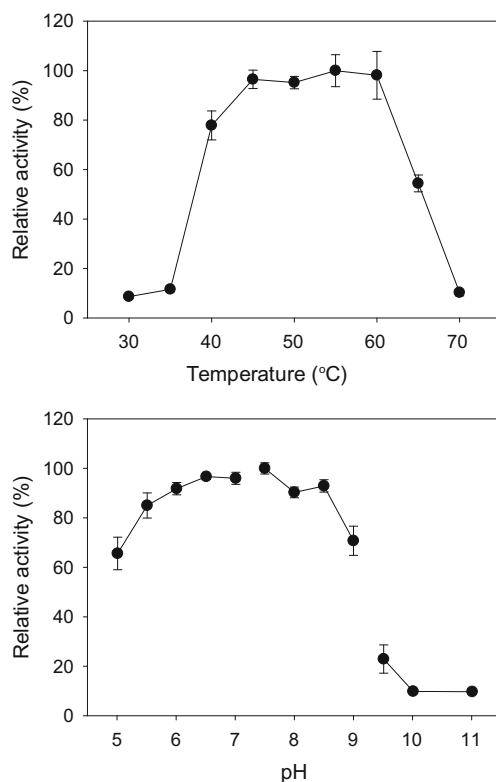


**Fig. 4** Optimal reaction (a) temperature and (b) pH of Aga16B. To assess the effect of temperature, the reactions were carried out at temperatures ranging from 30 to 70 °C in 20 mM Tris-HCl buffer (pH 7) for 30 min. To assess the effect of pH, the reactions were performed at 45 °C for 30 min in different buffers: 20 mM sodium phosphate (pH 5–7), 20 mM Tris-HCl buffer (pH 7.5–9), and 20 mM borate (pH 9.5–11)

(Fig. 4a). The optimal reaction pH of Aga16B was exhibited at pH 7.5, and Aga16B maintained approximately 93 % of its maximum activity over a broad range of pH 5.5 to 8.5 (Fig. 4b).

### Thermostability of Aga16B

Since the sol–gel transition (from sol to gel by cooling) temperature was determined to be ~35 °C, it is desired that the endo-type  $\beta$ -agarase used in the enzymatic liquefaction is stable over 35 °C; therefore, the thermostability of Aga16B was evaluated in this study. To determine the thermostability of Aga16B, the enzyme was preincubated at different temperatures (e.g., 40 to 65 °C) for different times (e.g., 0 to 120 min) prior to the enzymatic reaction of the preincubated Aga16B on 1 % (w/v) agarose at 45 °C for 30 min. The enzymatic activity of Aga16B was maintained at almost 100 % of its initial activity up to 50 °C of preincubation temperature for 120 min. When the preincubation temperature was increased to 55 °C and higher temperature, the enzymatic activity decreased to less than 20 % of its initial activity in fewer than 30 min of preincubation (Fig. 5).

### Optimal loading of Aga16B

To determine the optimal loading of Aga16B at the given enzymatic reaction conditions of a substrate loading of 1 % (w/v) agarose, pH 7.0, and 45 °C, initial reaction velocities with different loadings of Aga16B were compared (Fig. 6). The initial velocity obtained by Aga16B was increased until the loading of Aga16B increased to 42 U/g agarose. At a loading of Aga16B higher than 42 U/g agarose, the initial velocity of the enzymatic reaction was kept almost constant, even if the loading of Aga16B was increased (Fig. 6). In this study, the Aga16B loading of 42 U/g agarose was equivalent to 8 mg Aga16B/g agarose.

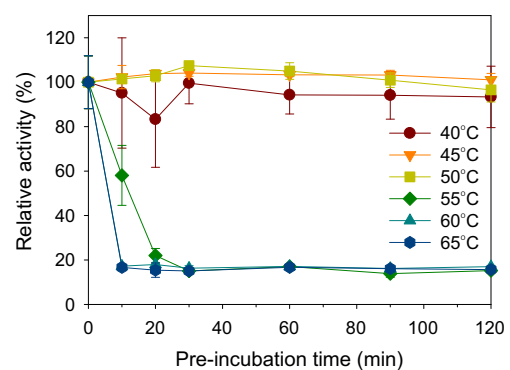


**Fig. 5** Thermostability of Aga16B. To measure thermostability of Aga16B, Aga16B was preincubated at 40–65 °C for 0–120 min prior to enzymatic reaction of Aga16B at 45 °C for 30 min

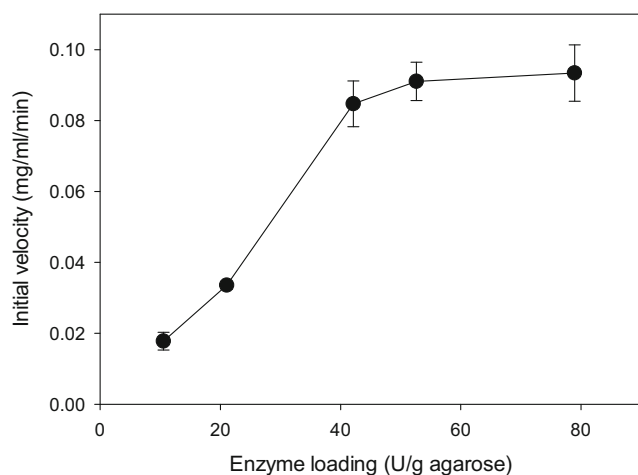


**Fig. 6** Effect of Agal6B loadings on the initial velocity. To assess the effect of Agal6B loading, the reaction conditions were carried out at different Agal6B loadings with 1 % (w/v) agarose in 20 mM Tris-HCl buffer (pH 7) at 45 °C

### Effect of metal ions on enzyme activity of Agal6B

The effect of metal ions on the enzymatic activity of Agal6B was tested in the presence of one of various metal ions with 1 % (w/v) agarose as the substrate (Table 1). Most of the ions revealed no effect on the enzymatic activity of Agal6B, except for  $\text{CuCl}_2$  and  $\text{FeCl}_2$ , with which the relative enzymatic activity of Agal6B significantly decreased to 76.6 and 82.6 % of its maximum activity, respectively (Table 1).

### Kinetic parameters of Agal6B

The kinetic parameters of Agal6B were calculated from the Lineweaver-Burk plot by using agarose as the substrate at a pH of 7.0 and 45 °C. These kinetic constants of Agal6B were then compared with those of other  $\beta$ -agarases belonging to GH16, originating from *Streptomyces coelicolor* (Temuujin

**Table 1** Effect of various metal ions on the relative activity of Agal6B

Salt	Relative activity %
Control <sup>a</sup>	100.0 ± 0.3
$\text{CuCl}_2$	76.6 ± 0.6
$\text{MgCl}_2$	99.1 ± 0.1
$\text{MnCl}_2$	93.4 ± 0.5
$\text{CaCl}_2$	96.5 ± 0.2
$\text{FeCl}_2$	82.6 ± 0.7
$\text{NH}_4\text{Cl}$	97.9 ± 0.1
KCl	96.8 ± 0.3
NaCl	93.0 ± 0.3

<sup>a</sup> The enzymatic activity with no metal ions was set as 100 %. Experimental data are mean ± standard deviation from triplicate experiments

et al. 2011), *Microbulbifer elongatus* JAMB-A7 (Ohta et al. 2004), and *Agarivorans albus* YKE-34 (Fu et al. 2009) (Table 2). The  $K_m$  value of Agal6B on agarose was 7.7 mg/ml, which was 38.5 times higher than that of AgaB34 (from *A. albus*) and 3.5 times higher than that of DagA (from *S. coelicolor*) (Table 2). The  $V_{max}$  value of Agal6B was 18.3 U/mg protein, which was 2.7 times lower than that of AgaB34. Compared to other  $\beta$ -agarases belonging to GH16, Agal6B showed the lowest value of  $k_{cat}$  (i.e., 20/s). Therefore, the catalytic efficiency (i.e.,  $k_{cat}/K_m$ ) of Agal6B was relatively low compared to those of other  $\beta$ -agarases of GH16 (Table 2).

### Mode of enzymatic action of Agal6B

To verify the mode of enzymatic action of Agal6B, the reaction products of agarose by Agal6B were analyzed by TLC (Fig. 7a) and HPLC (Fig. 7b). From the enzymatic reaction of agarose by Agal6B, two spots were mainly detected in TLC and the spot intensities increased with the reaction time (Fig. 7a). In the TLC analysis, monomeric sugars (i.e., AHG and galactose) and dimeric sugar (i.e., neoagarobiose) were not detected among the reaction products (Fig. 7a). By the HPLC analysis of the reaction products of agarose with Agal6B using the size-exclusion column, the degrees of polymerization 4 (DP4) and DP6 were detected as the major products, and DP8 was also detected as a minor product (Fig. 7b).

To identify the exact masses of the products of enzymatic reactions by Agal6B, MALDI-TOF/TOF MS analysis was performed (Fig. 8a). The exact masses of the major reaction products of agarose with Agal6B were measured as 653.2 and 959.3, which correspond to neoagarotetraose (DP4) and neoagarohexaose (DP6), respectively; meanwhile, neoagarooctaose (DP8) with a mass of 1265.4 was also detected as a minor product (Fig. 8a). By further analysis of the chemical structures of the major reaction products by tandem MS, neoagarotetraose and neoagarohexaose were confirmed (Fig. 8b, c). More specifically, the daughter ions produced from the precursor ions of neoagarotetraose and neoagarohexaose demonstrated that these reaction products consist of AHG and galactose, being bonded by alternating glycosidic linkages (Fig. 8b, c).

### Enzymatic liquefaction of agarose by Agal6B

To visually monitor the enzymatic liquefaction of agarose by Agal6B, the absorbance at 600 nm was measured after the enzymatic reaction of agarose (1 %, w/v) by Agal6B. After the enzymatic reaction, the absorbance (measured at 600 nm) of the postreaction mixture of Agal6B was similar to that of the 20 mM Tris-HCl buffer without agarose (Fig. 9). However, without enzymatic liquefaction, 1 % (w/v) agarose

**Table 2** Comparison of the kinetic parameters of Aga16B with the known agarases belonging to GH16

Agarase	Organism	Substrate	Product	$V_{\max}$ (U/mg protein)	$K_m$ (mg/ml)	$k_{\text{cat}}$ (/s)	$k_{\text{cat}}/K_m$ (/s/mg/ml)	Reference
Aga16B	<i>S. degradans</i> 2-40 <sup>T</sup>	Agarose	DP4, DP6	18.3	7.7	$2.0 \times 10^1$	$2.6 \times 10^1$	This study
AgaB34	<i>Agarivorans albus</i> YKW-34	Agarose	DP4	50.0	0.2	$4.1 \times 10^1$	$2.1 \times 10^2$	Fu et al. (2009)
DagA	<i>Streptomyces coelicolor</i>	Agarose	DP4, DP6	39.0	2.2	$9.5 \times 10^3$	$4.3 \times 10^3$	Temuujin et al. (2011)
AgaA7	<i>Microbulbifer elongatus</i> JAMB-A7	Agar	DP4	NA	3.0	$2.9 \times 10^6$	$9.6 \times 10^5$	Ohta et al. (2004)

NA not available

was solidified at room temperature, and its absorbance at 600 nm was significantly higher than that of the postenzymatic reaction mixture (Fig. 9).

## Discussion

In enzymatic liquefaction of agarose, the sol state of agarose in water can be more accessible to the enzymes than the gel state of agarose. In this study, we have evaluated a thermostable endo-type  $\beta$ -agarase, Aga16B, as an enzyme for the liquefaction of agarose. Since Aga16B revealed high thermostability up to 50 °C, which is over the sol–gel transition temperature (i.e., ~35 °C) of 1 % (w/v) agarose in water, Aga16B was considered to be feasible for the enzymatic liquefaction of agarose at a relatively high temperature.

Until now, for the efficient saccharification of agarose, chemical prehydrolysis using acetic acid or Tris-HCl buffer should be accompanied prior to the enzymatic saccharification for the chemical liquefaction of agarose (Kim et al. 2012, 2013; Lee et al. 2015; Yun et al. 2016). However, with chemical prehydrolysis, even-numbered AOSs are produced instead of NAOSs (Yang et al. 2009). As a result, agarotriose is produced as a by-product of the subsequent enzyme reaction by the exo-type  $\beta$ -agarase (Kim et al. 2012, 2013; Lee

et al. 2015). To hydrolyze agarotriose, an additional enzyme, ABG is required (Lee et al. 2014, 2015). Although the sugar yields increased significantly by the application of ABG, the agarose saccharification process has become more complicated and economically infeasible (Lee et al. 2015).

In this study, we demonstrated the enzymatic liquefaction of agarose using a thermostable endo-type  $\beta$ -agarase for the first time (Fig. 9). The sol–gel transition of agarose was found to occur at ~35 °C, and the gel structure of agarose became more rigid by cooling the agarose to ~5 °C (Fig. 3). By the enzymatic reaction of Aga16B, agarose decomposed to NAOS, with mainly DPs 4 and 6 (Figs. 7 and 8), and the postenzymatic reaction mixture did not turn to the gel state even at room temperature (Fig. 9). Through the enzymatic liquefaction of agarose using Aga16B, the chemical prehydrolysis using acid, requiring neutralization and the additional enzymatic reaction to hydrolyze agarotriose, can be avoided (Kim et al. 2013; Lee et al. 2015).

Aga16B originates from a marine bacterium, *S. degradans* 2-40<sup>T</sup>. In the  $\beta$ -agarase system of *S. degradans* 2-40<sup>T</sup>, Aga16B, belonging to GH16, was presumed to be involved in the initial step of agarose degradation by the endolytic hydrolysis of agarose to produce NAOSs (Ekborg et al. 2006). The exo-type  $\beta$ -agarase belonging to GH50 (e.g., Aga50D) acts on NAOSs for producing neoagarbiose (Kim et al. 2010;

**Fig. 7** **a** Time course analyses of reaction products of Aga16B by TLC and **b** overlaid HPLC chromatograms of reaction products of Aga16B. The reaction conditions were carried out with 1 % (w/v) agarose in 20 mM Tris-HCl buffer (pH 7) at 45 °C

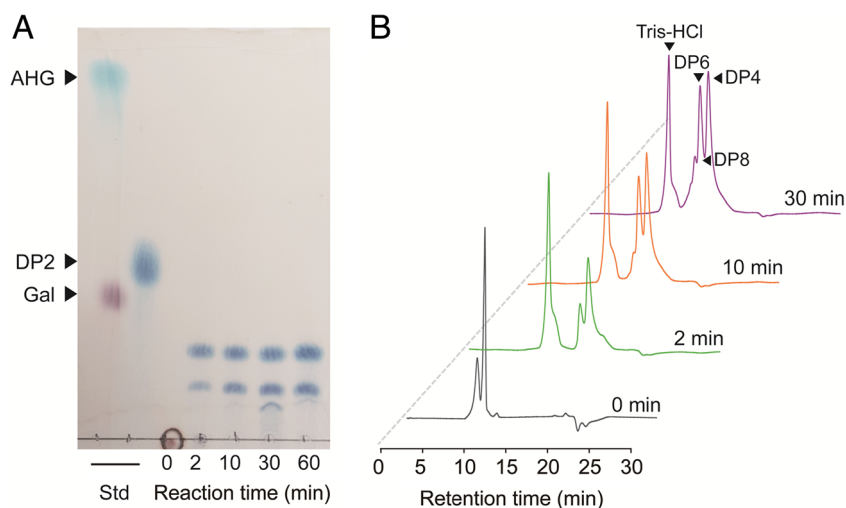


**Fig. 8** **a** Identification of reaction products of Aga16B by MALDI-TOF/TOF MS and **b, c** tandem MS analyses. The reaction conditions were carried out with 1 % (w/v) agarose in 20 mM Tris-HCl buffer (pH 7) at 45 °C

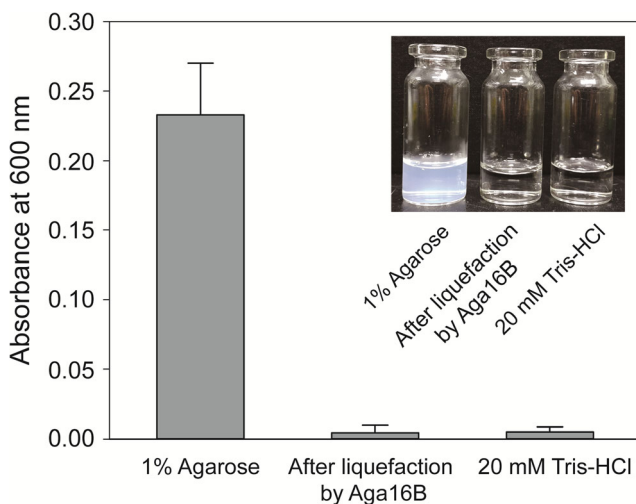
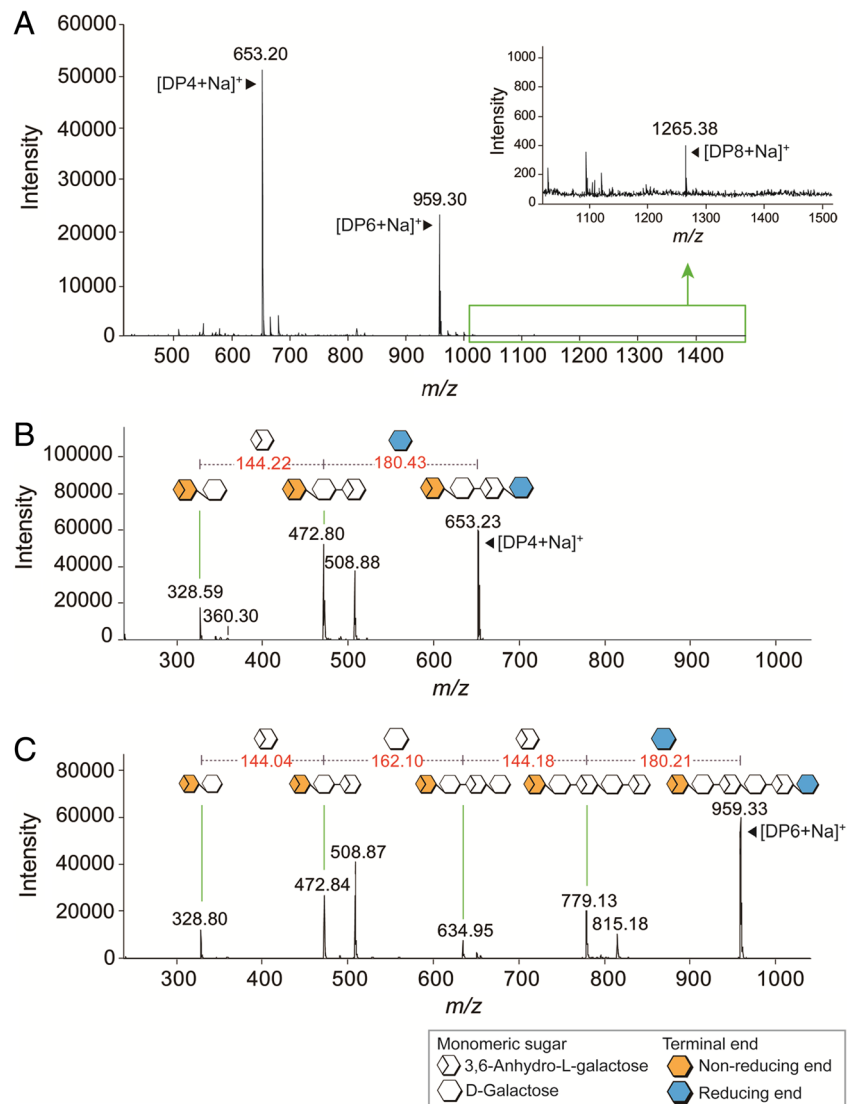


**Fig. 9** Enzymatic liquefaction of agarose by Aga16B. The turbidities of 1 % (w/v) agarose, the reaction products of Aga16B with 1 % (w/v) agarose, and 20 mM Tris-HCl buffer (pH 7) were compared by measuring their absorbances at 600 nm

Pluvinage et al. 2013). Finally, the neoagarobiose hydrolase (e.g., *SdNABH*), belonging to GH117, produces the monosaccharides D-galactose and 3,6-anhydro-L-galactose from neoagarobiose (Ha et al. 2011).

Among the characterized enzymes from the  $\beta$ -agarase system of *S. degradans* 2-40<sup>T</sup>, the optimal reaction temperatures for Aga50D and *SdNABH* were 30 and 42 °C, respectively (Ha et al. 2011; Kim et al. 2010); however, the optimal temperature for Aga16B ranged from 45 to 60 °C (Fig. 4a). Although some agarases belonging to GH16 showed optimal temperature up to 60 °C (Chi et al. 2014b; Lee et al. 2013; Ohta et al. 2004), most of these agarases significantly lost their activities at a temperature higher than 45 °C (Chi et al. 2014a; Fu et al. 2009; Kim et al. 2010; Temuujin et al. 2011; Zhang and Sun 2007). However, Aga16B showed thermostability in the preincubation at 50 °C for at least 120 min.

Meanwhile, the results of multiple amino acid sequence alignment revealed that Aga16B possesses the conserved catalytic



residues, Glu<sup>146</sup>, Glu<sup>151</sup>, and Asp<sup>148</sup>, which are commonly found in the enzymes belonging to GH16 (Allouch et al. 2003; Cui et al. 2014) (Fig. S1 in the Supplementary Material). From the aspect of the possible roles of these catalytic residues of Aga16B, Glu<sup>146</sup> and Glu<sup>151</sup> might act as nucleophiles and an acid/base, respectively, and Asp<sup>148</sup> might be important for maintaining the charged environment of catalytic amino acids. Furthermore, the catalytic motif (E[ILV]D[IVAF][VILMF]<sub>[0,1]E</sub>), which is prevalent in the enzymes of GH16, was also found to be conserved in Aga16B (Allouch et al. 2003) (Fig. S1 in the Supplementary Material).

In conclusion, the unique properties of Aga16B, such as the thermostability and the mode of action of producing DP4 and DP6, were exploited for the enzymatic liquefaction of agarose to replace the chemical prehydrolysis, which mainly relies on the use of an acid. Therefore, Aga16B can be effectively used as a liquefaction enzyme at a high temperature prior to enzymatic saccharification.

**Acknowledgments** This work was supported by a grant from the Ministry of Trade, Industry and Energy (10052721). Experiments were performed at the Korea University Food Safety Hall for the Institute of Biomedical Science and Food Safety.

#### Compliance with ethical standards

**Conflict of interest** The authors declare that they have no conflict of interest.

**Ethical statement** This article does not contain any studies with human participants or animals performed by any of the authors.

#### References

- Allouch J, Jam M, Helbert W, Barbeyron T, Kloareg B, Henrissat B, Czjzek M (2003) The three-dimensional structures of two  $\beta$ -agarases. *J Biol Chem* 278(47):47171–47180
- Armisen R (1991) Agar and agarose biotechnological applications. *Hydrobiologia* 221(1):157–166
- Armisen R, Galatas F (1987) Production, properties and uses of agar. In: McHugh DJ (ed) Production and utilization of products from commercial seaweeds. FAO Fisheries Technical Paper 288. FAO, Rome, Italy, pp. 1–57
- Brinker CJ, Scherer GW (2013) Sol–gel science: the physics and chemistry of sol–gel processing. Sol–gel processing. Academic Press, Cambridge, pp. 2–10
- Chi W-J, Chang Y-K, Hong S-K (2012) Agar degradation by microorganisms and agar-degrading enzymes. *Appl Microbiol Biotechnol* 94(4):917–930
- Chi W-J, Park DY, Seo YB, Chang YK, Lee S-Y, Hong S-K (2014a) Cloning, expression, and biochemical characterization of a novel GH16  $\beta$ -agarase AgaG1 from *Alteromonas* sp. GNUM-1. *Appl Microbiol Biotechnol* 98(10):4545–4555
- Chi W-J, Park J-S, Kang D-K, Hong S-K (2014b) Production and characterization of a novel thermostable extracellular agarase from *Pseudoalteromonas hodoensis* newly isolated from the West Sea of South Korea. *Appl Biochem Biotechnol* 173:1703–1716
- Cui F, Dong S, Shi X, Zhao X, Zhang X-H (2014) Overexpression and characterization of a novel thermostable  $\beta$ -agarase YM01-3, from marine bacterium *Catenovulum agarivorans* YM01<sup>T</sup>. *Mar Drugs* 12(5):2731–2747
- Ekborg NA, Taylor LE, Longmire AG, Henrissat B, Weiner RM, Hutcheson SW (2006) Genomic and proteomic analyses of the agarolytic system expressed by *Saccharophagus degradans* 2-40. *Appl Environ Microbiol* 72(5):3396–3405
- Fu XT, Pan C-H, Lin H, Kim SM (2009) Gene cloning, expression, and characterization of a  $\beta$ -agarase, agaB34, from *Agarivorans albus* YKW-3. *J Microbiol Biotechnol* 19(3):257–264
- Fujii T, Yano T, Kumagai H, Miyawaki O (2000) Scaling analysis on elasticity of agarose gel near the sol – gel transition temperature. *Food Hydrocoll* 14(4):359–363
- Ha SC, Lee S, Lee J, Kim HT, Ko H-J, Kim KH, Choi I-G (2011) Crystal structure of a key enzyme in the agarolytic pathway,  $\alpha$ -neogaroibiose hydrolase from *Saccharophagus degradans* 2-40. *Biochem Biophys Res Commun* 412(2):238–244
- Kim HT, Lee S, Lee D, Kim H-S, Bang W-G, Kim KH, Choi I-G (2010) Overexpression and molecular characterization of Aga50D from *Saccharophagus degradans* 2-40: an exo-type  $\beta$ -agarase producing neogaroibiose. *Appl Microbiol Biotechnol* 86(1):227–234
- Kim HT, Lee S, Kim KH, Choi I-G (2012) The complete enzymatic saccharification of agarose and its application to simultaneous saccharification and fermentation of agarose for ethanol production. *Bioresour Technol* 107:301–306
- Kim HT, Yun EJ, Wang D, Chung JH, Choi I-G, Kim KH (2013) High temperature and low acid pretreatment and agarase treatment of agarose for the production of sugar and ethanol from red seaweed biomass. *Bioresour Technol* 136:582–587
- Knutsen SH, Myslabodski DE, Larsen B, Usov AI (1994) A modified system of nomenclature for red algal galactans. *Bot Mar* 37(2):163–169
- Ko H-J, Park E, Song J, Yang TH, Lee HJ, Kim KH, Choi I-G, (2012) Functional cell surface display and controlled secretion of diverse agarolytic enzymes by *Escherichia coli* with a novel ligation-independent cloning vector based on the autotransporter YfaL. *Appl Environ Microbiol* 78(9):3051–3058
- Lahaye M, Yaphe W, Viet MTP, Rochas C (1989) <sup>13</sup>C-n.m.r. spectroscopic investigation of methylated and charged agarose oligosaccharides and polysaccharides. *Carbohydr Res* 190(2):249–265
- Lee Y, Oh C, Zoysa MD, Kim H, Wickramaarachchi WDN, Whang I, Kang D-H, Lee J (2013) Molecular cloning, overexpression, and enzymatic characterization of glycosyl hydrolase family 16  $\beta$ -agarase from marine bacterium *Saccharophagus* sp. AG21 in *Escherichia coli*. *J Microbiol Biotechnol* 23(7):913–922
- Lee CH, Kim HT, Yun EJ, Lee AR, Kim SR, Kim J-H, Choi I-G, Kim KH (2014) A novel agarolytic  $\beta$ -galactosidase acts on agarooligosaccharides for complete hydrolysis of agarose into monomers. *Appl Environ Microbiol* 80(19):5965–5973
- Lee CH, Yun EJ, Kim HT, Choi I-G, Kim KH (2015) Saccharification of agar using hydrothermal pretreatment and enzymes supplemented with agarolytic  $\beta$ -galactosidase. *Process Biochem* 50(10):1629–1633
- Li G, Sun M, Wu J, Ye M, Ge X, Wei W, Li H, Hu F (2015) Identification and biochemical characterization of a novel endo-type  $\beta$ -agarase AgaW from *Cohnella* sp. strain LGH. *Appl Microbiol Biotechnol* 99(23):10019–10029
- Medina-Esquivel R, Freile-Pelegrin Y, Quintana-Owen P, Yanez-Limon JM, Alvarado-Gil JJ (2008) Measurement of the sol–gel transition temperature in agar. *Int J Thermophys* 29(6):2036–2045
- Miller GL (1959) Use of dinitrosalicylic acid reagent for determination of reducing sugar. *Anal Chem* 31(3):426–428
- Nussinovitch A (1997) Hydrocolloid applications: gum technology in the food and other industries. Springer, New York, pp. 1–18

- Ohta Y, Hatada Y, Nogi Y, Miyazaki M, Li Z, Akita M, Hidaka Y, Goda S, Ito S, Horikoshi K (2004) Enzymatic properties and nucleotide and amino acid sequences of a thermostable  $\beta$ -agarase from a novel species of deep-sea *Microbulbifer*. Appl Microbiol Biotechnol 64(4):505–514
- Park DY, Chi W-J, Park J-S, Chang Y-K, Hong S-K (2015) Cloning, expression, and biochemical characterization of a GH16  $\beta$ -agarase AgaH71 from *Pseudoalteromonas hodoensis* H7. Appl Biochem Biotechnol 175(2):733–747
- Pluvinage B, Hehemann J-H, Boraston AB (2013) Substrate recognition and hydrolysis by a family 50 exo- $\beta$ -agarase, Aga50D, from the marine bacterium *Saccharophagus degradans*. J Biol Chem 288(39):28078–28088
- Sievers F, Wilm A, Dineen D, Gibson TJ, Karplus K, Li W, Lopez R, McWilliam H, Remmert M, Söding J, Thompson JD, Higgins DG (2011) Fast, scalable generation of high-quality protein multiple sequence alignments using Clustal Omega. Mol Sys Biol 7(1):539
- Temuujin U, Chi W-J, Lee S-Y, Chang Y-K, Hong S-K (2011) Overexpression and biochemical characterization of DagA from *Streptomyces coelicolor* A3(2): an endo-type  $\beta$ -agarase producing neoagarotetraose and neoagarohexaose. Appl Microbiol Biotechnol 92(4):749–759
- Wei N, Quarterman J, Jin Y-S (2013) Marine macroalgae: an untapped resource for producing fuels and chemicals. Trends Biotechnol 31(2):70–77
- Yang B, Yu G, Zhao X, Jiao G, Ren S, Chai W (2009) Mechanism of mild acid hydrolysis of galactan polysaccharides with highly ordered disaccharide repeats leading to a complete series of exclusively odd-numbered oligosaccharides. FEBS J 276(7):2125–2137
- Yun EJ, Lee S, Kim JH, Kim BB, Kim HT, Lee SH, Pelton JG, Kang NJ, Choi I-G, Kim KH (2013) Enzymatic production of 3,6-anhydro-L-galactose from agarose and its purification and *in vitro* skin whitening and anti-inflammatory activities. Appl Microbiol Biotechnol 97(7):2961–2970
- Yun EJ, Choi I-G, Kim KH (2015) Red macroalgae as a sustainable resource for bio-based products. Trend Biotechnol 33(5):247–249
- Yun EJ, Kim HT, Cho KM, Yu S, Kim S, Choi I-G, Kim KH (2016) Pretreatment and saccharification of red macroalgae to produce fermentable sugars. Bioresour Technol 199:311–318
- Zhang W-W, Sun L (2007) Cloning, characterization, and molecular application of a  $\beta$ -agarase gene from *Vibrio* sp. strain V134. Appl Environ Microbiol 73(9):2825–2831